A&A 522, A98 (2010)
DOI: 10.1051/0004-6361/201014741

Astronomy & Astrophysics

uvby–β photometry of solar twins

The solar colors, model atmospheres, and the $T_{\rm eff}$ and metallicity scales[⋆,⋆⋆]

J. Meléndez[1,2], W. J. Schuster[3], J. S. Silva[3], I. Ramírez[4], L. Casagrande[4], and P. Coelho[5]

[1] Centro de Astrofísica da Universidade do Porto, Rua das Estrelas, 4150-762 Porto, Portugal
e-mail: jorge@astro.up.pt
[2] Departamento de Astronomia do IAG/USP, Universidade de São Paulo, Rua do Matão 1226, Cidade Universitária, 05508-900 São Paulo, SP, Brasil
e-mail: jorge@astro.iag.usp.br
[3] Observatorio Astronómico Nacional, Universidad Nacional Autónoma de México, Apartado Postal 877, Ensenada, B.C., CP 22800, Mexico
e-mail: schuster@astrosen.unam.mx
[4] Max Planck Institute for Astrophysics, Postfach 1317, 85741 Garching, Germany
[5] Núcleo de Astrofísica Teórica, Universidade Cruzeiro do Sul, R. Galvão Bueno, 868, Liberdade, 01506-000 São Paulo, Brasil

Received 7 April 2010 / Accepted 5 July 2010

ABSTRACT

Aims. Solar colors have been determined on the *uvby*–β photometric system to test absolute solar fluxes, to examine colors predicted by model atmospheres as a function of stellar parameters ($T_{\rm eff}$, log g, [Fe/H]), and to probe zero-points of $T_{\rm eff}$ and metallicity scales.
Methods. New *uvby*–β photometry is presented for 73 solar-twin candidates. Most stars of our sample have also been observed spectroscopically to obtain accurate stellar parameters. Using the stars that most closely resemble the Sun, and complementing our data with photometry available in the literature, the solar colors on the *uvby*–β system have been inferred. Our solar colors are compared with synthetic solar colors computed from absolute solar spectra and from the latest Kurucz (ATLAS9) and MARCS model atmospheres. The zero-points of different $T_{\rm eff}$ and metallicity scales are verified and corrections are proposed.
Results. Our solar colors are $(b-y)_\odot = 0.4105 \pm 0.0015$, $m_{1,\odot} = 0.2122 \pm 0.0018$, $c_{1,\odot} = 0.3319 \pm 0.0054$, and $\beta_\odot = 2.5915 \pm 0.0024$. The $(b-y)_\odot$ and $m_{1,\odot}$ colors obtained from absolute spectrophotometry of the Sun agree within 3-σ with the solar colors derived here when the photometric zero-points are determined from either the STIS HST observations of Vega or an ATLAS9 Vega model, but the $c_{1,\odot}$ and $\beta_\odot$ synthetic colors inferred from absolute solar spectra agree with our solar colors only when the zero-points based on the ATLAS9 model are adopted. The Kurucz solar model provides a better fit to our observations than the MARCS model. For photometric values computed from the Kurucz models, $(b-y)_\odot$ and $m_{1,\odot}$ are in excellent agreement with our solar colors independently of the adopted zero-points, but for $c_{1,\odot}$ and $\beta_\odot$ agreement is found only when adopting the ATLAS9 zero-points. The $c_{1,\odot}$ color computed from both the Kurucz and MARCS models is the most discrepant, probably revealing problems either with the models or observations in the u band. The $T_{\rm eff}$ calibration of Alonso and collaborators has the poorest performance (∼140 K off), while the relation of Casagrande and collaborators is the most accurate (within 10 K). We confirm that the Ramírez & Meléndez *uvby* metallicity calibration, recommended by Árnadóttir and collaborators to obtain [Fe/H] in F, G, and K dwarfs, needs a small (∼10%) zero-point correction to place the stars and the Sun on the same metallicity scale. Finally, we confirm that the c_1 index in solar analogs has a strong metallicity sensitivity.

Key words. Sun: fundamental parameters – stars: atmospheres – stars: fundamental parameters – stars: solar-type

1. Introduction

Photometry in the *uvby*–β system (Strömgren 1963; Crawford 1966) is well suited to the determination of basic stellar atmospheric parameters for F-, G-, and K-type stars through the color indices $(b–y)$, $m_1 = (v–b) - (b–y)$ and $c_1 = (u–v) - (v–b)$. Several empirical calibrations exist in the literature to transform $(b–y)$ or β to $T_{\rm eff}$ (e.g. Alonso et al. 1996, 1999; Clem et al. 2004; Ramírez & Meléndez 2005b, hereafter RM05b; Holmberg et al. 2007; Casagrande et al. 2010), while the m_1 index can be used to determine [Fe/H] in dwarfs (e.g. Strömgren 1964; Gustafsson & Nissen 1972; Olsen 1984; Schuster & Nissen 1989; Malyuto 1994; Haywood 2002; Martell & Laughlin 2002; Martell & Smith 2004; Ramírez & Meléndez 2005a, hereafter RM05a; Twarog et al. 2007; Holmberg et al. 2007) and giants (e.g. Bond 1980; Arellano Ferro & Mantegazza 1996; Hilker 2000; Ramírez & Meléndez 2004; Calamida et al. 2007, 2009), as reviewed by Árnadóttir et al. (2010). The evolutionary stage of stars can be determined using the c_1 index together with other *uvby* color indices (e.g. Crawford 1975; Olsen 1984; Nissen & Schuster 1991; Schuster et al. 2004; Twarog et al. 2007).

Since there are many difficulties in observing the Sun with the same instrumentation as we observe other stars (e.g. Stebbins & Kron 1957; Gallouëtte 1964; Clements & Neff 1979; Tueg 1982; Lockwood et al. 1992), the Sun cannot be used to set the zero-points of transformations between color indices and fundamental stellar parameters. Accurate transformations are important in many areas of astrophysics. For example, in the study of the primordial lithium abundance, an accurate $T_{\rm eff}$ scale is needed to compare the Li abundance of metal-poor stars with that obtained from Big Bang Nucleosynthesis (e.g. Meléndez et al. 2010a; Sbordone et al. 2010). The terrestrial planet signatures found in the chemical composition of

⋆ Based on observations collected at the H. L. Johnson 1.5 m telescope at the Observatorio Astronómico Nacional at San Pedro Mártir, Baja California, México.
⋆⋆ Tables 1–3 and 5 are only available in electronic form at http://www.aanda.org

the Sun (Meléndez et al. 2009, hereafter M09; Ramírez et al. 2009, hereafter R09; Ramírez et al. 2010) shows that for accurate comparisons between the Sun and stars an accurate temperature scale must be used in the determination of chemical abundances. Although there is inconclusive evidence about whether the Sun is too metal-rich with respect to stars of similar age and Galactic orbit (Haywood 2008; Holmberg et al. 2009) implying that the Sun could have been born in the inner part of the Galaxy (Wielen et al. 1996), this apparent offset between the Sun and stars could be partly due to zero-point errors in the photometric metallicity scale (see e.g. Table 3 of Árnadóttir et al. 2010, for systematic differences between spectroscopic and photometric metallicities). Furthermore, we note that zero-point errors in the $T_{\rm eff}$ scale, as well as errors in the metallicity scale, would introduce systematic errors in the ages of stars determined from isochrones.

According to their similarity to the Sun, stars can be classified as "solar-type stars" (late F to early K stars), "solar analogs" (G0−G5 dwarfs with solar metallicity within ~a factor of 2−3), and "solar twins" (stars almost identical to the Sun) (e.g. Secchi 1868; Cayrel de Strobel 1996; Soderblom & King 1998; M09). Many works have used either solar-type stars or solar analogs to infer solar colors to improve or check the effective temperature scale, the performance of model atmospheres, and the absolute flux calibration of the Sun (e.g. Pettit & Nicholson 1928; Kuiper 1938; Stebbins & Whitford 1945; Stebbins & Kron 1957; Johnson 1962; Kron 1963; van den Bergh 1965; Croft et al. 1972; Olsen 1976; Schuster 1976; Barry et al. 1978; Hardorp 1978, 1980a,b; Clements & Neff 1979; Cayrel de Strobel et al. 1981; Neckel & Labs 1981; Chmielewski 1981; Tueg & Schmidt-Kaler 1982; Magain 1983; Taylor 1984; Mitchell & Schuster 1985; Neckel 1986; Vandenberg & Poll 1989; Gray 1992, 1995; Straizys & Valiauga 1994; Taylor 1994; Cayrel de Strobel 1996; Colina et al. 1996, hereafter C96; Hauck & Kunzli 1996; Bessell et al. 1998; Mironov et al. 1998; Sekiguchi & Fukugita 2000; Meléndez & Ramírez 2003; RM05b; Holmberg et al. 2006; Pasquini et al. 2008; Rieke et al. 2008; Casagrande et al. 2010).

Solar twins have spectra almost identical to the Sun (Cayrel de Strobel 1996), hence are better suited to setting the zero-points of fundamental calibrations, especially since they are found without assuming a priori a temperature scale, but their identification is based purely on a model-independent analysis of their spectra with respect to a solar spectrum obtained with the same instrumentation. However, until a few years ago only one solar twin was known (18 Sco; Porto de Mello & da Silva 1997; Soubiran & Triaud 2004). The situation has changed dramatically with the identification of many stars similar to the Sun (Meléndez et al. 2006, hereafter M06; Meléndez & Ramírez 2007, hereafter MR07; Takeda et al. 2007, hereafter T07; Takeda & Tajitsu 2009, hereafter T09; M09; R09; Baumann et al. 2010, hereafter B10). It is now feasible to use solar twins with accurately determined stellar parameters to test the predictions of model atmospheres and the accuracy of empirical photometric calibrations. In the present work, we perform this study for the widely used *uvby–β* system.

2. Photometric observations

2.1. Selection of the sample

Before starting our systematic survey of stars similar to the Sun in the Hipparcos catalogue, we performed pilot observations of solar-twin candidates to test our selection criteria. Our pilot study (M06) found zero-point offsets in our $T_{\rm eff}$ scale (RM05b). We therefore applied small corrections to the solar colors predicted by RM05b to increase our chances of finding stars resembling the Sun. In particular, we searched for solar twins around the Tycho color $(B-V)_{\rm T} = 0.7225$ instead of $(B-V)_{\rm T} = 0.689$ predicted by our earlier color-$T_{\rm eff}$ relations (RM05b). Our improved $T_{\rm eff}$ scale (Casagrande et al. 2010) indeed corrected the zero-point problem, and now predicts a solar $(B-V)_{\rm T} = 0.730$, in good agreement with our tentative correction.

The main parameters used to select solar-twin candidates from the Hipparcos catalogue were parallaxes and $(B-V)_{\rm T}$ colors. Additional criteria used (when available) were other optical-infrared colors (e.g. $V_{\rm T}-K$, $b-y$), photometric variability, information on multiplicity, previous literature values for [Fe/H] (obtained from an updated version of the Cayrel de Strobel et al. 2001, catalogue), rotation, and chromospheric activity. We found initially about one hundred stars satisfying our selection criteria within 75 pc. We later expanded our search to cover the whole Hipparcos catalogue, increasing our sample by about 1/3.

2.2. Observations and data reduction

The *uvby–β* data presented here in Table 1 for the solar twins were taken using the H. L. Johnson 1.5 m telescope at the San Pedro Mártir Observatory, Baja California, México (hereafter SPM), and the same six-channel *uvby–β* photoelectric photometer as for the northern observations of Schuster & Nissen (1988, hereafter SN), for all the *uvby–β* observations of Schuster et al. (1993, hereafter SPC), the northern data of very-metal-poor stars by Schuster et al. (1996), the *uvby–β* data for very-metal-poor stars in Table 1 of Schuster et al. (2004), and the *uvby–β* data for high-velocity and metal-poor stars in Table 1 of Schuster et al. (2006). The new *uvby–β* values for solar twins included here in Table 1 were taken during three observing runs in November 2007 (8 nights), April 2008 (7 nights), and September 2008 (4 nights).

The *uvby–β* solar-twin data were taken and reduced using techniques very nearly the same as for SN and SPC (see these previous papers for more details). The four-channel *uvby* section of the SPM photometer is really a spectrograph-photometer that employs exit slots and optical interference filters to define the bandpasses. The grating angle of this spectrograph-photometer was calibrated using a cadmium lamp at the beginning of each observing run to position the spectra on the exit slots to within about ±1 Å. Whenever possible, extinction-star observations were made nightly over an air-mass range of at least 0.8 (see Schuster & Parrao 2001; also Schuster et al. 2002), and spaced throughout each night several "drift" stars were observed symmetrically with respect to the local meridian (two hours east and then two hours west). Using these observations, the atmospheric extinction coefficients and time dependences of the night corrections could be obtained for each of the nights of observation (see Grønbech et al. 1976). Finding charts were employed at SPM to confirm identifications of the program stars and to select regions for the "sky" measurements. As for previous studies, such as SN and SPC, the program stars were observed at SPM to at least 50 000 counts in all four channels of *uvby* and to at least 30 000 counts for the two channels centered at H*β*. For all program stars, the sky background was measured until its contributing error was equal to or smaller than the error in the stellar count. At SPM, an attempt was made to obtain three or more independent *uvby* observations for each of the program stars, i.e. photometric observations during at least three independent nights; this aim was achieved, or exceeded, for all solar twins except HIP 75923 and HIP 77883 for which we obtained two observations each.

As for the SN and SPC catalogues, all data reduction was carried out following the precepts of Grønbech et al. (1976) using computer programs kindly loaned by T. Andersen (see Parrao et al. 1988). At SPM, the *uvby–β* standard stars observed were taken from the same lists as for the previous catalogues, and are mostly secondary standards from the catalogues of Olsen (1983, 1984). The reduction programs create a single instrumental photometric system for each observing run, including nightly atmospheric extinctions and night corrections with linear time dependences. Then transformation equations from the instrumental to the standard systems of V, $(b–y)$, m_1, c_1, and β are obtained using all standard stars observed during that observing period. The equations for the transformation to the standard *uvby–β* system are the linear ones of Crawford & Barnes (1970) and Crawford & Mander (1966). Small linear terms in $(b–y)$ are included in the standard transformation equations for m_1 and c_1 to correct for bandwidth effects in the v filter. Our y measurements were transformed onto the V system of Johnson et al. (1966).

Thirty-six *uvby–β* standard stars were employed during the observing run of November 2007 providing instrumental photometric errors ranging from 0.002 mag in $(b–y)$ to 0.009 mag in c_1, and errors in the transformations to the standard photometric system from 0.004 to 0.011 mag, respectively. For April 2008, these values were for 33 standard stars, 0.002−0.010 mag, and 0.005−0.013 mag, respectively, and for September 2008, for 35 standard stars, 0.002−0.008 mag, and 0.006−0.009 mag, respectively. Instrumental and transformation errors in the magnitude V and in the indices m_1 and β were always intermediate in value between those given above.

2.3. The catalogue

Table 1 presents the *uvby–β* catalogue for the 73 solar-twin candidates observed at SPM. Column 1 lists the Hipparcos number; Col. 2 gives the HD (or BD) number, Col. 3 the V magnitude on the standard Johnson UBV system; and Cols. 4–6 and 9, the indices $(b–y)$, m_1, c_1 and β on the standard systems of Olsen (1983, 1984), which are essentially the systems of Crawford & Barnes (1970) and Crawford & Mander (1966) with north-south systematic differences corrected. Columns 7, 8, and 10 give N_V, N_{uvby}, and N_β, the total numbers of independent V, *uvby*, and β observations.

A very small subset of our photometric observations was made through light cirrus clouds in the absence of moonlight. It has been well documented (e.g. SN; Olsen 1983) that observations in the indices $b–y$, m_1, c_1, and β made with simultaneous multichannel photometers are not affected in any significant way by light (or even moderate) cirrus, while the V magnitude, obtained from only the y band, is affected. For this reason, a few of the solar twins, such as HIP 60314, HIP 74389, and HIP 118159, have fewer independent observations of the V magnitude than the indices.

2.4. Comparisons with other photometric data

We searched for *uvby–β* photometry in the General Catalogue of Photometric Data (Mermilliod et al. 1997; Hauck & Mermilliod 1998) and found data for 23 solar-twin candidates and 12 solar analogs (observed by ourselves spectroscopically for other projects). The photometry of these 35 stars is given in Table 2.

The accuracy of *uvby–β* photometry obtained at SPM has been extensively tested (e.g. SN; Arellano Ferro et al. 1990; Schuster et al. 1993, 1996), and we illustrate below that our solar-twin photometry is also in excellent agreement with the literature, in all cases with mean differences well below 0.01 mag. There are 12 stars in common between our sample and previous work. The average difference (ours – literature) in $(b–y)$ is only −0.001 (σ = 0.004). Our V Johnson photometry is also in good agreement, with a mean difference (ours – literature) of only +0.001 (σ = 0.006). The colors m_1 and c_1 also compare well, with a difference (ours – literature) of only +0.002 (σ = 0.006) and +0.006 (σ = 0.015).

Considering the excellent agreement between the photometry available in the literature and in our own data sets, and considering the previously shown accuracy and precision of the SPM *uvby–β* photometry, we conclude that both data sets, of Tables 1 and 2, provide solar-color indices very close to the standard *uvby–β* system.

3. The solar-color indices

Our observations comprise the largest photometric data set yet taken of stars very similar to the Sun in the *uvby–β* system. Adding other photometry available in the literature and using our own accurate stellar parameters (M09; R09; Meléndez et al. 2010b, hereafter M10b), and taking into account the variations in colors with $T_{\rm eff}$, log g and [Fe/H], we can infer the "solar" colors by interpolating them to the stellar parameters of the Sun: $T_{\rm eff}$ = 5777 K, log g = 4.44, and [Fe/H] = 0.00 (e.g. Cox 2000; Gray 2005; RM05b).

The quality of our stellar parameters (M06; MR07; M09; R09; M10b) is very high because both the Sun (reflected light of asteroids) and the solar twins were observed with the same instrumentation during the same observing runs, and all data reduction and analysis were performed in an identical way. Our spectra have typically a resolution of 60 000 and $S/N \sim 200$ for stars observed with the 2.7 m telescope at McDonald and $S/N \sim$ 450 for stars observed with 6.5 m Magellan Clay telescope at Las Campanas. Errors as low as ~25 K in $T_{\rm eff}$, 0.04 dex in log g, and 0.025 dex in [Fe/H] can be obtained in the best cases, and abundance ratios with errors as low as 0.01−0.02 dex have been obtained with the above data, showing that the Sun is a star with a peculiar chemical composition (M09; R09). Additional spectra available in the literature for solar-twin candidates were analyzed by B10 using similar techniques. The spectra are from HARPS observations available at the ESO archive and from the S^{4}N database (Allende Prieto et al. 2004)[1]. In both cases, a solar spectrum taken with the same instrumentation was employed in the differential analysis.

The stellar parameters were determined homogeneously by our own group (M06; MR07; M09; R09; M10b; B10) using Kurucz model atmospheres and a line-by-line differential analysis with respect to the Sun. The $T_{\rm eff}$, log g, [Fe/H], and microturbulence were determined iteratively until both the differential excitation equilibrium of FeI lines and the differential ionization balance of FeI and FeII, were achieved. The microturbulence was also determined simultaneously, by requiring no dependence of the iron abundance (from FeI lines) on the reduced equivalent width.

[1] S^{4}N: Spectroscopic Survey of Stars in the Solar Neighborhood; available online at http://hebe.as.utexas.edu/s4n/

Table 4. Global fits for color = $A + B\,(T_{\rm eff} - 5777) + C\,(\log g - 4.44) + D$ [Fe/H].

Color	A	Error	B	Error	C	Error	D	Error	σ (fit)	Solar colors
$b-y$	0.4105	0.0005	–1.2737e-4	9.2777e-6			0.049813	0.004753	0.0046	0.4105 ± 0.0015
m_1	0.2122	0.0006	–1.1405e-4	1.1657e-5	0.05051	0.00936	0.125539	0.005877	0.0056	0.2122 ± 0.0018
c_1	0.3319	0.0018			–0.11223	0.02658	0.124344	0.016006	0.0165	0.3319 ± 0.0054
β	2.5915	0.0008	4.5183e-5	1.5840e-5	–0.03241	0.01192	0.034604	0.007492	0.0061	2.5915 ± 0.0024

Since our solar-twin sample spans a relatively narrow range in atmospheric parameters relative to the Sun, in principle simple linear fits of color versus (vs.) each parameter ($T_{\rm eff}$, log g, and [Fe/H]) would provide sufficiently good estimates of the solar colors. As suggested by the referee, a global fit (e.g. Mitchell & Schuster 1985) to all stellar parameters (color = $f(T_{\rm eff}$, log g, [Fe/H])) would be preferable due to the mutual interdependence of the stellar parameters. Fortunately our sample includes also solar analogs covering a broader range in colors and stellar parameters than the solar twins, so that the dependence on the different stellar parameters can be well determined by a global fit. The following formula was employed:

$$\text{color} = A + B\,(T_{\rm eff} - 5777) + C\,(\log g - 4.44) + D\,[\text{Fe/H}]. \quad (1)$$

The advantage of this equation is that A will give us directly the solar color, while its uncertainty could be determined from the error in A or from the scatter of the fit.

From our sample of stars, we selected a group of solar twins with $T_{\rm eff}$, log g, and [Fe/H] within 100 K, 0.1 dex, and 0.1 dex of the solar parameters[2] given above. To perform a more robust global fit, we extended our solar twin sample with solar analogs covering a range in $T_{\rm eff}$, log g, and [Fe/H]. Thus, to explore the metallicity dependence of the colors, we selected a sample of solar analogs with the same constraints in $T_{\rm eff}$ and log g, but covering a broader range in metallicity (–0.4 < [Fe/H] < –0.1 dex, +0.1 < [Fe/H] < +0.4 dex). In a similar way, to improve the fit to $T_{\rm eff}$, we selected a group of solar analogs with the same constraints on log g and [Fe/H] as the solar twins, but with $T_{\rm eff}$ in the range ($5617 < T_{\rm eff} < 5677$ K, $5877 < T_{\rm eff} < 5937$ K). Finally, to fit the trend with log g, we used a sample of solar analogs with the same constraints on $T_{\rm eff}$ and [Fe/H] as the solar twins, but covering a broader range in log g ($4.29 \le \log g < 4.34$ dex, $4.54 \le \log g < 4.59$ dex).

The stellar parameters were taken from our work on solar twins (M06; MR07; M09; R09; M10b; B10) and complemented in some cases with other accurate values available in the literature (Valenti & Fischer 2005, hereafter VF05; Luck & Heiter 2006, hereafter LH06, T07; Sousa et al. 2008, hereafter S08, T09). The adopted stellar parameters for the solar twins and solar analogs are given in Table 3.

The global fits to (b–y) had only three outliers, HIP 7245, HIP 81512, and HIP 88427, which seem too red in (b–y) for their $T_{\rm eff}$ and [Fe/H]. Using the Karataş & Schuster (2010) intrinsic-color calibration, we find that these three stars may be slightly reddened ($E(b-y) \sim 0.015$–0.023), although we have to bear in mind that the accuracy of the reddening calibration is of the same order[3]. These stars were removed from the global fits. The results from the fits are presented in Table 4 and in Figs. 1–4, where filled circles represent the solar twins and open circles the solar analogs across a broader range of stellar parameters.

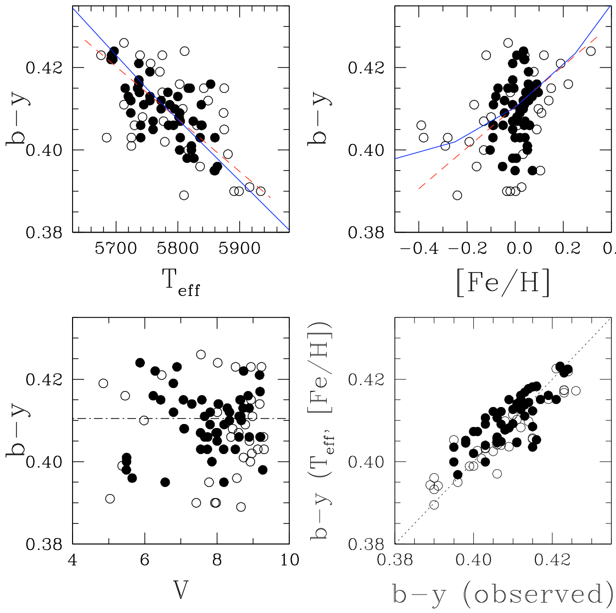

Fig. 1. (b–y) vs. $T_{\rm eff}$ (*upper left panel*), [Fe/H] (*upper right panel*), and V magnitude (*lower left panel*, with a dot-dashed line at $(b-y)_\odot$). The results of the global fit vs. the observed $(b-y)$ color is presented in *the lower right panel*, with the dotted line indicating equality. Solar twins and solar analogs are represented by filled and open circles, respectively. The dependences of the fit on $T_{\rm eff}$ and [Fe/H] are shown by dashed lines, while the relative predictions of MARCS models (normalized to our inferred solar colors) are shown by solid lines.

3.1. The (b–y) solar color

The global fit of (b–y) (Fig. 1 and Table 4) shows strong dependences on $T_{\rm eff}$ (at the 14-σ level) and [Fe/H] (10-σ). There is no dependence (within the errors) on log g, therefore this parameter was excluded from the global fit. The star-to-star scatter from the fit is only 0.005 mag, which is what is expected from the observational uncertainties (0.004–0.006 mag).

The standard error (s.e.) in the solar color was obtained from the observed star-to-star scatter and the number of data-points (s.e. = $\sigma/\sqrt{\text{sample size}}$). The error in $(b–y)_\odot$ (and the other solar colors) was conservatively adopted as three times the standard error. Thus, we propose

$$(b-y)_\odot = 0.4105\ (\pm 0.0015). \quad (2)$$

A plot of (b–y) vs. V magnitude can help us to reveal whether fainter (i.e., more distant) stars bias the above derived solar color, either in our solar-twin or our solar-analog samples, so it was not considered in the global fits.

[2] Strictly speaking, a solar-twin star must be identical to the Sun within the observational uncertainties. Our definition based on derived stellar parameters is simply more practical because it is less dependent on the quality of the stellar and solar spectra available.

[3] The star HIP 79186 also seems reddened according to the Karataş & Schuster (2010) calibration, but the stellar parameters of this star ($T_{\rm eff}$, log g, and [Fe/H]) = (5709 K, 4.27 dex, –0.12 dex) (R09) do not fall

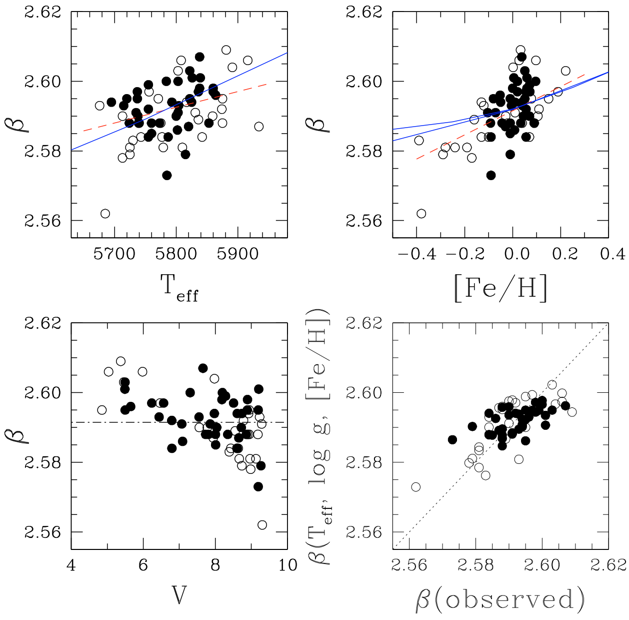

Fig. 2. β vs. $T_{\rm eff}$ (*upper left panel*), [Fe/H] (*upper right panel*), and V magnitude (*lower left panel*). The results of the global fit vs. the observed β color is presented in *the lower right panel*. Symbols are as in Fig. 1, except that two curves are presented for MARCS models: the shallower curve is the one computed by us while the other one is from O09. Neither curve is able to explain the low β colors observed for [Fe/H] < −0.2.

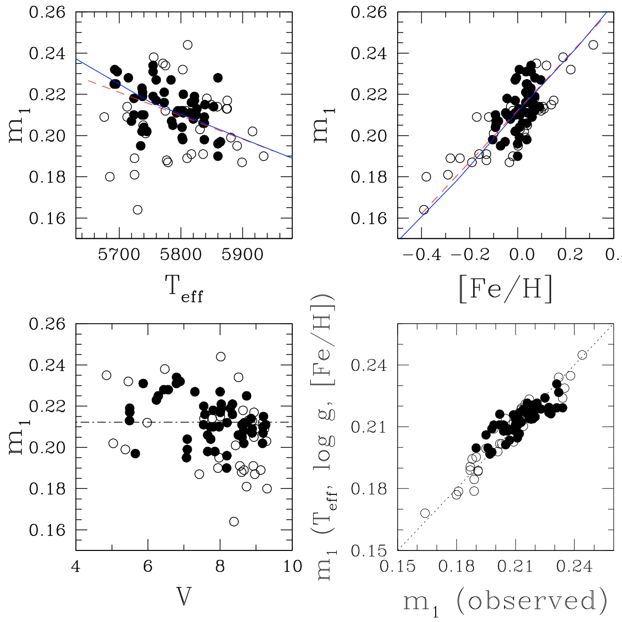

Fig. 3. m_1 vs. $T_{\rm eff}$ (*upper left panel*), [Fe/H] (*upper right panel*), and V magnitude (*lower left panel*). The results of the global fit vs. the observed m_1 color is presented in *the lower right panel*. Symbols are as in Fig. 1.

due to possible interstellar reddening. This plot is shown in the lower left panel of Fig. 1. As can be seen, there is no trend with V magnitude. A linear fit of $(b–y)$ vs. V, indeed shows a zero slope within the errors (slope = 0.0003 ± 0.0008). We note that most stars of the sample used in the global fit are brighter than $V = 9$, i.e. closer than ~68 pc. Even the faintest stars ($V \sim 9.3$) extend only to ~78 pc. According to NaI interstelar absorption maps, very little NaI absorption is detected for distances up to ~80 pc from the Sun (Lallement et al. 2003; Welsh et al. 2010). Thus, most of our sample is not expected to be significantly affected by interstellar absorption. As already mentioned above, the few stars that show some small sign of interstellar reddening were not included in the global fits.

3.2. The β solar color

The global fit of β shows a dependence on $T_{\rm eff}$, log g, and [Fe/H] (Table 4). Interestingly, the strongest dependence is with [Fe/H] (slope significant at the 5-σ level), while the dependence with both $T_{\rm eff}$ (2.9σ) and log g (2.7σ) is only at the 3-σ level. In Fig. 2, we show the dependence of the β color index with respect to $T_{\rm eff}$ and [Fe/H]. The scatter from the fit is 0.006 mag, which is compatible with the observational errors in β.

The adopted β solar color is

$$\beta_\odot = 2.5915\ (\pm 0.0024). \quad (3)$$

Although there is a clear trend of β vs. V magnitude (Fig. 2), it is not related to reddening because the β index is not affected by interstellar absorption. The bright stars ($V < 6$) that are causing the trend are within ~17 pc, hence they are not reddened. The bright ($V < 6$) solar twins and analogs falling systematically above the derived $\beta_\odot$, are stars hotter than the Sun, or more metal-rich than the Sun (or both), and therefore with a β color systematically higher than solar because β increases with both increasing metallicity and $T_{\rm eff}$. We note that the trend seen in nearby stars for β is not present in $(b–y)$ because this color has opposite trends with $T_{\rm eff}$ and [Fe/H]. Thus, by performing a deeper solar-twin survey than previous works, we avoided systematic biases (such as selecting mainly hotter and more metal-rich stars) that might have been present if only brighter stars were studied.

3.3. The m_1 solar color

It is well known that the m_1 color correlates very well with metallicity (see references in the introduction), and this is clearly shown in Table 4, where according to the global fit the dependence on [Fe/H] is significant at the 21-σ level. The second most important parameter is $T_{\rm eff}$ (10σ), but log g also produces an important dependence (slope significant at the 5-σ level).

The tight correlation between m_1 and [Fe/H] is shown in Fig. 3. The star-to-star scatter from the global fit is only 0.006 mag, which is compatible with the observational uncertainties. The m_1 solar color recommended for the Sun is

$$m_{1,\odot} = 0.2122\ (\pm 0.0018). \quad (4)$$

3.4. The c_1 solar color

In Fig. 4, we show the relation between c_1 and log g, which is significant at the 4-σ level. As already noticed in the literature (e.g. Twarog et al. 2002; Önehag et al. 2009, hereafter O09), the c_1 index in late G dwarfs has a sensitivity to metallicity. Our global fit (Table 4) confirms the dependence on [Fe/H], which is actually more significant (8-σ) than the dependence on log g (Fig. 4).

The predicted c_1 solar color from the global fit is

$$c_{1,\odot} = 0.3319\ (\pm 0.0054). \quad (5)$$

The star-to-star scatter in the global fit is 0.0165, which is considerably larger than the observational errors (0.009–0.013)

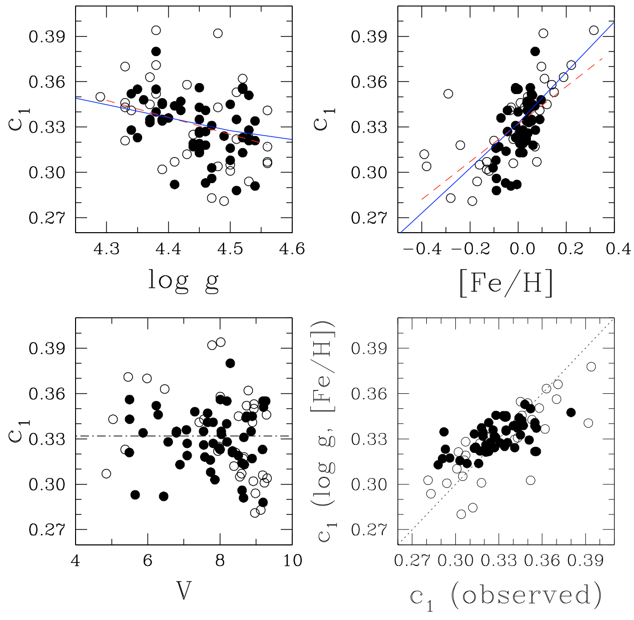

Fig. 4. c_1 vs. log g (*upper left panel*), [Fe/H] (*upper right panel*) and V magnitude (*lower left panel*). The results of the global fit vs. the observed c_1 color is presented in *the lower right panel*. Symbols are as in Fig. 1.

for the c_1 index. Following the suggestions of the referee, we explored whether this index is particularly sensitive to either anomalies in the chemical composition or the microturbulence velocities.

Previous works show the effects of C and N upon the Strömgren 4-color *uvby* filter-measurements, via the NH and CN bands. For example, it seems that the NH band at 3360A affects the u measurements while CN affects the v measurements. Thus, the c_1 color that depends on both u and v should be affected by abundance anomalies (Bond & Neff 1969; Bond 1974; Zacs et al. 1998; Grundahl et al. 2000, 2002; Schuster et al. 2004; Yong et al. 2008). In this context, it would be important to assess whether the small abundance anomalies in the solar chemical composition (M09; R09), in particular the difference between the highly volatile elements (C, N, O) and Fe, may affect the *uvby* colors. As discussed by Stromgren et al. (1982), variations in the He abundance may also affect the c_1 index. Although the Hyades c_1 anomaly for stars with $(b-y)$ close to solar was found initially to be $\Delta c_1 \sim 0.03{-}0.04$ (Hyades – field stars, or Hyades – Coma), it seems that the anomaly may only amount to Δc_1 = 0.024−0.025 after instrumental effects are corrected (Joner & Taylor 1995). Another important parameter affecting the colors may be microturbulence (Conti & Deutsch 1966; Nissen 1981).

To test the above effects, synthetic spectra were computed for solar twins with variations in Δ[C, N, O/Fe] = −0.05 dex (M09), $\Delta v_{\rm micro}$ = +0.1 km s^{-1} (most solar twins and close solar analogs have $v_{\rm micro}$ within ±0.1 km s^{-1} of the solar value), and an increase of 10% in the He abundance (by number). Fluxes were computed with the code SYNTHE (Kurucz & Avrett 1981; Sbordone et al. 2004; Kurucz 2005) using ATLAS12 model atmospheres (Kurucz 1996, 2005; Castelli 2005) computed for the different aforementioned assumptions. The atomic line list adopted in the spectral computations is based on the compilations by Coelho et al. (2005) and Castelli & Hubrig (2004), and the molecules C_2, CH, CN, CO, H_2, MgH, NH, OH, SiH, and SiO from Kurucz (1993) were included. The change in He does not significantly affect the c_1 index (<0.001 mag), but the change in microturbulence increases c_1 by +0.0035 mag, while the change in C, N, O increases c_1 by +0.003 mag[4]. Thus, small changes in chemical composition and microturbulence may help to explain the extra scatter seen in the global fit. Casagrande et al. (in prep.) demonstrate that the Strömgren system is not only sensitive to [Fe/H], but that it is possible to obtain information about the [α/Fe] ratio using *uvby* photometry. The Δc_1 anomaly in the Hyades could be due to the effect of metallicity on c_1. According to Friel & Boesgaard (1992), Hyades has an iron abundance 0.18 dex higher than Coma, which according to Table 4 corresponds to Δc_1 = +0.022 mag, which is very close to the Hyades anomaly relative to Coma (0.024−0.025 mag) (Joner & Taylor 1995).

4. Comparison with previous empirical determinations

As can be seen in Table 5 (lower part), our inferred $(b-y)$, m_1, c_1, and β solar colors agree well (within 1-σ) with most earlier empirical results. However, previous determinations of solar colors have much lower control and homogeneity in $T_{\rm eff}$, log g, and [Fe/H], thus in some cases the agreement (within the error bars) could be due to fortuitous compensations of $T_{\rm eff}$, log g, and [Fe/H] effects on colors, or due to large errors in other studies.

Several previous works (Saxner & Hammarback 1985; Gray 1992; Edvardsson et al. 1993; Casagrande et al. 2010) give $(b-y)_\odot$ values that agree with ours within 0.005 mag, but other determinations are either too blue (Cayrel de Strobel 1996; Clem et al. 2004; RM05b; Holmberg et al. 2006) or too red (Gehren 1981). A previous empirical result for $\beta_\odot$ (Saxner & Hammarback 1985, $\beta_\odot$ = 2.591 ± 0.005) is in excellent agreement with our value (2.5915 ± 0.0024). Previous determinations of $m_{1,\odot}$ and $c_{1,\odot}$ (Clem et al. 2004; Holmberg et al. 2006) also agree with ours within the errors, but note that the errors given by Holmberg et al. (2006) are very large (0.03 and 0.07 for m_1 and c_1, respectively), so their solar colors cannot be used to perform stringent tests of model atmospheres and the temperature and metallicity scales.

Although our inferred solar colors agree with previous determinations based on solar-type stars, our values based on solar twins should be preferred because of their more accurate and precise stellar parameters, resulting in correspondingly accurate and precise inferred solar colors. We use our "solar" colors below to test absolutely calibrated solar spectra, model atmospheres and the $T_{\rm eff}$ and metallicity *uvby*–β scales.

5. Comparison with measurements on reflected (asteroid) solar spectra

Olsen (1976) measured the $\beta_\odot$ color of reflected solar light from asteroids, which seems justifiable because the β index should be largely independent of the wavelength dependence of the albedo. His measurement ($\beta_\odot$ = 2.5955 ± 0.0024) is in good agreement (within 1-σ) with our inferred value ($\beta_\odot$ = 2.5915 ± 0.0024). Olsen (1976) did not measure the solar $(b$–$y)$, but indirectly estimated $(b-y)_\odot$ from a color transformation using $\beta_\odot$. His $(b-y)_\odot$ = 0.390 ± 0.004 disagrees with ours (0.4105 ± 0.0015), but this is probably due to the errors introduced by his adopted transformation from β to $(b$–$y)$. Using the $(b-y)_0$–β intrinsic

[4] The changes in $(b-y)$ and m_1 due to changes in He, CNO, and microturbulence are even smaller than for c_1.

color calibration of Karataş & Schuster (2010), the $\beta_{\odot} = 2.5955$ from Olsen (1976) indeed implies that $(b–y)_{\odot} = 0.4062$, in good agreement with our $(b–y)_{\odot}$. Using the same transformation, our $\beta_{\odot} = 2.5915$ gives $(b–y)_{\odot} = 0.4089$.

Unfortunately, direct measurements of the $(b–y)$, m_1 and c_1 color indices for reflected solar spectra are not very useful because of the color of the asteroid albedos[5]. A comparison with solar colors inferred from absolute spectrophotometry of the Sun is presented below.

6. Comparison with synthetic colors

Our accurate and precise colors inferred for the Sun can be used to test the performance of theoretical solar flux models and the quality of absolute solar flux measurements. However, additional ingredients enter the computation of synthetic colors, namely the adopted set of filters and the flux/magnitude zero-points adopted. We discuss them in the following.

Since intermediate-band Strömgren filters are centered on specific spectral features, a correct characterization of the total throughout becomes crucial for generating synthetic colors (e.g. Lester et al. 1986, O09). To test the influence of the filter transmission curves on our results, we computed *uvby* indices using two different sets of pass-bands, the original ones of Crawford & Barnes (1970) and a set that should be more representative of the SPM observations (Bessell 2005).

The β index is defined as the ratio of the flux measured through narrow (half-width of about 30 Å) and wide (about 150 Å) profiles both centered on the Hβ line. In this case, the (212, 214) filter transmission curves (Crawford & Mander 1966), the photomultiplier sensitivity, the atmospheric transmission, and the reflectivity of aluminum given in Castelli & Kurucz (2006) were used to generate the total T_{β} throughout, according to the prescriptions of the beta.forcd program at the Kurucz website[6]. Indices calculated using T_{β} define the natural system β', which should be transformed using a set of equations to agree to the standard system β defined by the observations of Crawford & Mander (1966). For the filter set (212, 214), the transformation equation is $\beta = 0.248 + 1.368\,\beta'$ (Crawford & Mander 1966).

In principle, to mimic the *uvby–β* observations presented here, synthetic photometry should reproduce the SPM instrumental system, and the same transformation equations should then be applied to generate the standard system. In practice, this can hardly be done, since the SPM instrument is a six-channel spectrophotometer, and we follow the approach normally adopted in the literature, i.e. of reproducing the standard system directly, by fixing the zeropoints using Vega. In Sect. 2.4, we have shown the excellent agreement between our observations and other photometric measurements, meaning that the transformation from the instrumental to the standard system is indeed accurate, we therefore expect our approach to return meaningful synthetic colors.

The spectral energy distribution adopted for Vega and its observed indices also affect the outcome of synthetic photometry in the process of establishing the zeropoints of a photometric system (e.g. Casagrande et al. 2006). We used a spectrum obtained with the STIS spectrograph onboard the HST (Bohlin 2007) of resolution $\mathcal{R} = 500$, which enables the highest accuracy (∼1%) measurements achievable to date, and adopted the following averaged values for Vega: $(b-y) = 0.003$, $m_1 = 0.157$, $c_1 = 1.088$ and $\beta = 2.904$ from Hauck & Mermilliod (1998). If we had adopted the colors of Vega given in Crawford et al. (1972), the differences would have amounted to 0.001 mag at most.

Despite the complications posed by the pole-on and rapidly rotating nature of Vega, the effects on the blue part of the spectrum are expected to be small or negligible (e.g. Casagrande et al. 2006; Bohlin 2007, and references therein). It is more relevant that we use the observed HST spectrophotometry of Vega; additional comments on this issue are made in the following subsections.

6.1. Colors from Kurucz and MARCS models

Although synthetic *uvby–β* colors computed using earlier MARCS and Kurucz models are found in the literature (see Table 5), we feel it appropriate to make our comparisons using the most recent releases available (Castelli & Kurucz 2004; Gustafsson et al. 2008). In addition, as we have already mentioned, different ingredients enter the computation of synthetic colors, and we differ from most of the previous works in that we use an observed spectrum of Vega to define the zeropoints. In principle, this should be the best approach for replicating observations and for a correct comparison of solar flux models and absolute measurements with the colors determined from our solar twins. This choice mimics the observational approach, and the successes or failures of synthetic colors depend mostly on the quality of the solar input spectra. In practice, the situation is less clear, as we discuss further below and in Sect. 6.2.

When computing synthetic colors from theoretical models, the use of a model atmosphere to describe also Vega may have the advantage of (partly) compensating for model inaccuracies by including these in the zero-points.

We performed this exercise by taking from the Kurucz website the latest ATLAS9 model fluxes for Vega and the Sun; because of the internal consistency of this approach, it should also determine which set of filters should be used. For the colors of the Sun we obtain $(b-y) = 0.413$, $m_1 = 0.236$ and $c_1 = 0.297$ using the filters of Crawford & Barnes (1970), and $(b-y) = 0.406$, $m_1 = 0.214$, $c_1 = 0.303$ for the Bessell (2005) filters. While $(b–y)_{\odot}$ is reproduced with the two set of filters, the latter set of filters provides results that are more comparable to our measured $m_{1,\odot}$ and $c_{1,\odot}$, and therefore in the following we consider only the Bessell (2005) passbands. The effect of instead using those of Crawford & Barnes (1970) can be easily estimated from the above differences.

The resolution of the spectra used to generate synthetic colors may also in principle affect the results. We tested ATLAS9 model fluxes for Vega and the Sun at various resolutions ranging from $\mathcal{R} = 500\,000$ to 200 and verified that for various combinations of these, differences in $(b–y)$, m_1 and c_1 always lie below 0.001 mag[7].

However, for $\mathcal{R} \lesssim 2000$ the synthetic β index scales differently for Vega and the Sun, i.e. even if synthetic spectra of the same resolution are used for the two stars, the value obtained for β depends on $\mathcal{R}$ to an extent that may vary from a few millimagnitudes up to several hundredths of a magnitude. For example, using high resolution ATLAS9 spectra for both Vega and the

[5] Although the colors of the Sun measured using asteroids may be affected, our spectroscopic analysis based on high-resolution spectra should not because we measure the flux relative to the adjacent continuum for narrow spectral lines

[6] http://kurucz.harvard.edu/programs/COLORS

[7] The Castelli & Kurucz (2004) grid of fluxes has a resolution varying from 150 to 250 in the wavelength region of interest, and for this reason we took instead model fluxes at higher resolution from the Kurucz website.

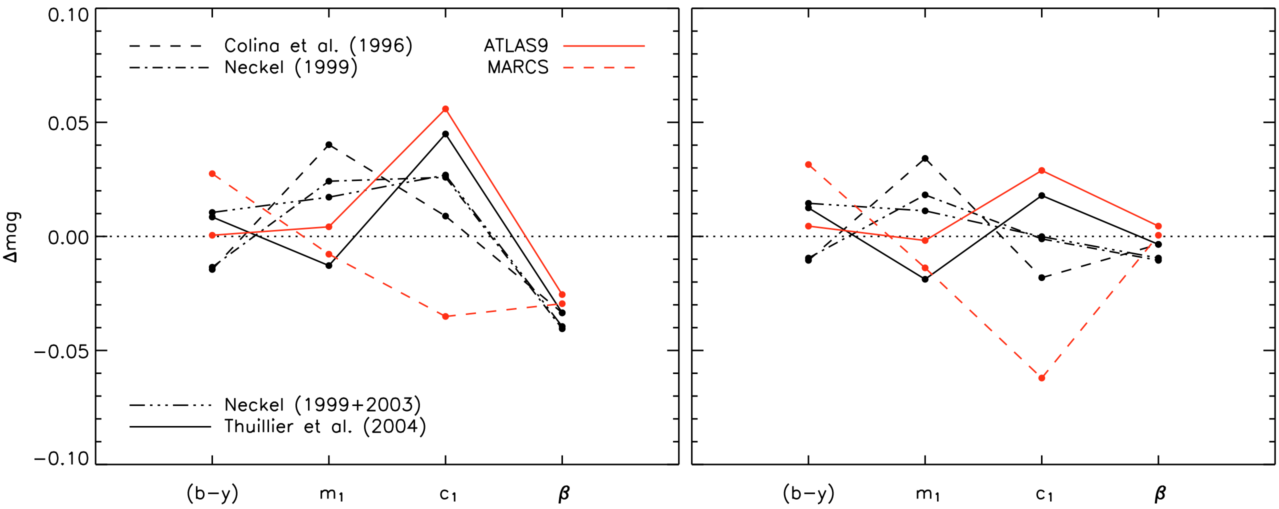

Fig. 5. Comparison between solar and synthetic colors obtained from different spectra. *Left panel*: using Vega STIS observations to set the zero-points. *Right panel*: using ATLAS9 Vega model for the same purpose. Δmag = our derived solar colors minus the synthetic ones.

Sun, we obtain $\beta = 2.587$, which is in good agreement with our solar value. Using instead synthetic spectra of Vega and the Sun at $\mathcal{R} = 500$ sampled at the same wavelength points, we obtain $\beta = 2.601$ from which we estimate a (model-dependent) correction of 0.014 mag when working at this low $\mathcal{R}$.

Because of this limitation on the STIS resolution of the Balmer line, the β indices computed for Table 5 have been obtained as follows: the solar spectra were downgraded to $\mathcal{R} = 500$, sampled at the same wavelength points as the STIS spectrum, and the aforementioned correction was then applied. Using instead a high resolution ATLAS9 spectrum of Vega to define the zero-points does not require a downgrade to the resolution of the solar spectra, and the β indices are changed by −0.030 mag (i.e. are bluer). We verified that for the other Strömgren indices the STIS resolution is high enough. The effect of using an ATLAS9 model flux of Vega to set the zero-points amounts to −0.004, 0.006, and 0.027 mag for the $(b{-}y)$, m_1, and c_1 indices, respectively. In Fig. 5, synthetic colors obtained with these two choices for Vega, i.e. STIS vs. ATLAS9, are compared.

If the STIS spectrum of Vega is used, the Kurucz solar flux returns a value of $(b{-}y)$ in excellent agreement with our observed value, whereas a considerably bluer color is obtained with MARCS. The greater accuracy of the Kurucz with respect to the MARCS solar flux in b and y bands can be noticed also from the spectrophotometric comparison presented in Edvardsson (2008). For m_1, the Kurucz model is still in better agreement than the MARCS, one being slightly bluer and the other redder with respect to our $m_{1,\odot}$. The same bluer and redder performance is also obtained for c_1, although both models provide a rather poor match. The β index is similar for both models and considerably redder than our $\beta_\odot$.

In general, the ATLAS9 solar flux model performs better than the MARCS model, but they both have problems in reproducing $c_{1,\odot}$ (in opposite directions) and $\beta_\odot$ (both systematically redder). Changing to the ATLAS9 flux of Vega to set the zero-points has a negligible impact on $(b{-}y)$ and m_1, but brings the theoretical β index in almost perfect agreement in both cases. For the c_1 index, only the ATLAS9 result is helped by this choice, and this could partly stem from compensating errors in the ATLAS9 models of Vega and the Sun.

In Table 5, we also show the color indices computed by O09 using MARCS models (also for the flux of Vega) and the passbands of Crawford & Barnes (1970). Their $(b{-}y)$ agrees with our synthetic one, but their m_1 and c_1 colors are somewhat redder and bluer, respectively, in a way that is consistent with the different passbands they adopted. The c_1 solar color computed by O09 is in excellent agreement (within 1-σ) with our $c_{1,\odot}$.

6.2. Colors from solar spectra

We computed $(b{-}y)$, m_1, c_1, and β indices using the absolute measurements of solar spectra by C96, Neckel (1999, hereafter N99), and Thuillier et al. (2004). The spectrum of Rieke et al. (2008) was not employed because of its very low resolution ($R \sim 100$). The STIS Vega observations and the ATLAS9 Vega model were again used to define the zero points.

The C96 composite spectrum represents both satellite (Woods et al. 1996) and ground (Neckel & Labs 1984) observations below and above 4100 Å. While its $(b{-}y)$ is redder, m_1 is considerably bluer, and c_1 is in good agreement with our solar values. Not unexpectedly, the same conclusions about $(b{-}y)$ and m_1 hold for the N99 atlas, which is an update of the Neckel & Labs (1984) measurements included in C96. However, Neckel (2003, hereafter N03) noticed a possible systematic error in those absolute measurements and provides a simple analytical formula for correction, after which $(b{-}y)$ and m_1 are in closer agreement with our solar values. Thuillier et al. (2004) published two composite solar reference spectra assembled using space measurements during distinct solar activity levels; differences concern only the m_1 and c_1 indices in a negligible manner (a few millimagnitudes only), and therefore in Table 5 the averaged values of the two are given. Thuillier et al. (2004) provide closer agreement than previous spectra in $(b{-}y)$ and m_1, but their c_1 is considerably bluer.

Thus, while on average $(b{-}y)$ and m_1 are in agreement with our solar values, there is the tendency for c_1 to be considerably bluer. The β indices were computed following the same prescriptions as in the previous section and are systematically redder. Switching to the model flux of Vega solves most of the discrepancies for these two indices, with the synthetic values being now distributed at the red and blue sides of our solar colors (see the right panel of Fig. 5). It is not obvious why a model flux for Vega also brings absolute solar flux measurements into closer agreement with our empirical solar colors. While the measured spectra of Vega should be superior to any model of it, we can speculate about possible reasons for this not being true over the full wavelength range. The difference STIS vs. ATLAS9 amounts to few millimagnitudes in $(b\text{–}y)$ and m_1, but is considerable in c_1 and β, and those differences could reflect measurement problems in the u band and the issue already mentioned about the spectral resolution around the Balmer line.

In the wavelength range of interest to us, the accuracy of the solar absolute fluxes is on the order of 5−3% from data acquired in space (C96, Thuillier et al. 2004) and probably lower for ground-based data measurements. The culprit could thus be inaccuracy in solar flux measurements rather than in Vega! For the sake of computing indices, we are not interested in the absolute flux scale, but rather in the relative accuracy of measuring the shape of the solar spectral energy distribution. This accuracy is rather difficult to assess, but the above differences provide an idea of the complexity associated with this kind of measurement, and the corresponding rather large uncertainties. In addition, the choice for Vega and the set of filters used also affect the analysis, introducing systematic errors.

In this section, we have presented various issues concerning synthetic solar colors, which are often taken for granted when comparing observed vs. synthetic colors. While the comparison with a specific solar-flux measurement has limited significance, with appropriate choices for Vega, it is comforting that there are no large systematic trends between our solar colors and these observations taken together. Thus, our solar colors can help considerably in establishing the necessary reliability of synthetic colors.

6.3. Testing the effects of changes in T_{eff}, log g, and [Fe/H] on synthetic MARCS colors

As discussed in the previous sections, our *uvby*–β solar colors are useful for testing absolute solar spectra and the performance of model atmospheres, as well as checking the subtleties in the transformation from fluxes to synthetic colors. Since our solar twins and analogs span a range in $T_{\rm eff}$, log g, and [Fe/H], we can also use them to test how well model atmospheres predict the relative change of colors due to variations in atmospheric parameters.

For this test, we used relative fluxes predicted by the MARCS models, normalizing the results to our "observed" solar colors. As shown in Figs. 1–4, where the relative variation in the MARCS $(b\text{–}y)$, β, m_1, and c_1 colors are shown by solid lines, there is a satisfactory overall *relative* agreement between MARCS models and both the solar twins and solar analogs. The only clear discrepancy is in the predicted metallicity variation in β (Fig. 2), which is much shallower than observed. We also checked whether the MARCS β colors computed by O09 solve this problem (Fig. 2), but although they do help to slightly alleviate the discrepancy (the Önehag et al. β colors are slightly steeper than ours), they also do not match the low β indices observed below [Fe/H] ~ -0.2. It would be important to observe more metal-poor solar analogs to confirm whether we have detected a potential problem in the line formation of Hβ.

The strong variation in c_1 with metallicity for G-type stars (Twarog et al. 2002, Fig. 4, see also O09) is reproduced well by the MARCS models (as already demonstrated by O09 for somewhat cooler dwarfs), so it can potentially be used to estimate [Fe/H] in solar metallicity and metal-rich solar analogs.

Our tests provide confidence in the relative variation in stellar fluxes with atmospheric parameters as predicted by the MARCS models, at least in the atmospheric parameter space studied here.

Table 6. $\Delta\ T_{\rm eff}$ needed to correct the zeropoint of the most recent $T_{\rm eff}$ scales.

$\Delta\ T_{\rm eff}$ (K)	Reference
	$(b-y)$
+137	Alonso et al. (1996)
+85	Gratton et al. (1996)
+118	Blackwell & Lynas-Gray (1998)
+68	Clem et al. (2004)
+109	RM05b
+48	Holmberg et al. (2007)
+10	Casagrande et al. (2010)
	β
+130	Alonso et al. (1996)

7. The zero-point of the $T_{\rm eff}$ scale

Our solar $(b\text{–}y)$ color can also be used to estimate how well different $T_{\rm eff}$ scales reproduce the solar value of $T_{\rm eff}$ (5777 K). Different color-$T_{\rm eff}$ relations in the literature have been employed to obtain the $T_{\rm eff}$ for our $(b-y)_\odot$, and these values have then been subtracted from the solar effective temperature. These differences, shown in Table 6, are the zero-point corrections needed to place different $T_{\rm eff}$ calibrations on the same $T_{\rm eff}$ scale as the Sun. As can be seen, the $T_{\rm eff}$ scale by Casagrande et al. (2010) seems the most accurate, with a negligible offset of only 10(±10) K with respect to the Sun, which is much smaller than the offset (109 K) of our earlier $T_{\rm eff}$ calibration (RM05b).

The widely used $T_{\rm eff}$ $(b\text{–}y)$ scale of Alonso et al. (1996) is too cool by 137 K. Thus, the elemental chemical abundances determined using this scale (e.g. Israelian et al. 1998; Chen et al. 2000; Reddy et al. 2003; Allende Prieto et al. 2004; Jonsell et al. 2005) may be systematically incorrect by as much as 0.14 dex (e.g. for V from VI lines and for N from NH lines), albeit the impact on abundance ratios [X/Fe] should be smaller (and in a few cases mostly cancel) for lines of low to moderate excitation potential because of the compensating impact of the iron abundance obtained from FeI lines; however, for abundances obtained from lines of high excitation potential (e.g. CI, NI, OI, PI, SI) the impact could be as high as 0.2 dex. Thus, inaccurate temperature scales may be one of the reasons why the small peculiarities in the solar chemical composition (M09; R09) have not been discovered in the past (Ramírez et al. 2010).

Zero-point errors in $T_{\rm eff}$ also affect stellar ages inferred from isochrones. For example, for an offset of 130 K and using Y^2 isochrones (Demarque et al. 2004), a systematic offset as high as 1.5−2 Gyr may result for a solar analog.

8. The zero-point of the metallicity scale

Árnadóttir et al. (2010) made a critical evaluation of different metallicity calibrations for dwarf stars in the *uvby* system, finding zero-point offsets in many of these metallicity scales, ranging from −0.17 dex (Nordström et al. 2004) to +0.33 (O09), although the latter is a purely theoretical calibration intended to test model atmospheres and not for application to real stars. After extensive testing for potential problems in different metallicity calibrations, such as trends in the Δ[Fe/H] residuals (spectroscopic-photometric) with [Fe/H], $(b-y)$, c_0, and m_0,

Table 7. Δ [Fe/H] needed to correct the zero-point of different *uvby* metallicity scales.

Δ [Fe/H] This work	Δ [Fe/H] Árnadóttir et al. (2010)	Reference
+0.06, +0.05	+0.11 ± 0.34	Olsen (1984)
+0.05	+0.06 ± 0.16	Schuster & Nissen (1989)
−0.04	+0.00 ± 0.18	Haywood (2002)
+0.07	+0.05 ± 0.13	Martell & Laughlin (2002)
+0.07	+0.06 ± 0.21	Martell & Smith (2004)
+0.04	+0.04 ± 0.14	RM05a
+0.09	+0.08 ± 0.16	Holmberg et al. (2007)
+0.37	+0.33 ± 0.30	O09

Árnadóttir et al. (2010) find that the calibrations by RM05a has the best overall performance, albeit with a small (0.04 dex) zero-point offset.

The zero-point offset cannot be overstated, especially when comparing the Sun to the stars (Gustafsson 2008), because offsets in the zero-point of the metallicity scale could make the Sun appear abnormal (see Haywood 2008; Gustafsson et al. 2010, and references therein for a discussion about apparent anomalies in the solar metallicity).

Our solar colors can be used to check the zero-point of different metallicity calibrations, by computing [Fe/H] for our inferred solar colors and subtracting these metallicities from the solar metallicity ([Fe/H] = 0). Those differences, which are the zero-point corrections needed to place different metallicity calibrations on the same metallicity scale as the Sun, are shown in Table 7, along with the offsets found by Árnadóttir et al. (2010) for a broad range of colors and metallicities.

Most metallicity calibrations do require a correction to place them on the same metallicity scale as the Sun. In particular, the RM05a metallicity calibration recommended by Árnadóttir et al. (2010) to derive [Fe/H] from Strömgren photometry, needs a zero-point correction of +0.04 dex. This offset is identical to the offset found by Árnadóttir et al. (2010) using a sample spanning a much broader range in $T_{\rm eff}$. We are currently revising the metallicity calibration employed in the GCS survey (Nordström et al. 2004; Holmberg et al. 2007) and plan to assess the apparent anomalously high metallicity of the Sun with a new accurate metallicity scale (Casagrande et al., in prep.).

9. Conclusions

New *uvby*–β photometry has been presented for solar-twin candidates observed at the SPM observatory. Comparisons with existing Strömgren photometry shows that our data are in excellent agreement (to better than 0.01 mag) with previous observations.

Using accurate spectroscopically derived stellar parameters, the *uvby*–β photometry for the solar twins, and also for solar analogs covering a wider range in metallicities, the solar colors $(b-y)_\odot = 0.4105 \pm 0.0015$, $m_{1,\odot} = 0.2122 \pm 0.0018$, $c_{1,\odot} = 0.3319 \pm 0.0054$, and $\beta_\odot = 2.5915 \pm 0.0024$ have been inferred.

As discussed in the manuscript, our solar-twin data have provided stringent constraints on absolute fluxes, the performance of model atmospheres, and the zero-points of temperature and metallicity scales. In particular, we show that the widely used Alonso et al. (1996) (b–y) calibration is too cool by ~140 K, while our new $T_{\rm eff}$ calibration (Casagrande et al. 2010) has a negligible zero-point offset (10 ± 10 K). Regarding model atmospheres, the Kurucz ATLAS9 solar model provides a closer fit of our solar colors than the MARCS 2008 solar model. The relative variation in colors with stellar parameters seem to be reproduced well by MARCS models, except for the metallicity variation in the β index, which is flatter than observed in solar twins and solar analogs, thus suggesting that there are existing limitations on the modeling of Balmer lines.

We are pursuing photometric observations of our solar-twin sample in other photometric systems, to perform similar evaluations of absolute fluxes, model atmospheres, and fundamental calibrations in astrophysics.

Acknowledgements. We thank A. Önehag and B. Gustafsson for computing the solar color indices (in the O09 system) given in Table 5, and also by comments on our results. W.J.S. is very grateful to the DGAPA-PAPIIT (UNAM) (projects Nos. IN101495, and IN111500) and to CONACyT (México) (projects Nos. 1219–E9203, 27884E, and 49434F) for funding which permitted travel and also the maintenance and upgrading of the *uvby*–β photometer. J.M. would like to acknowledge support from Fundação para a Ciência e a Tecnologia (FCT, Portugal) in the form of a grant (PTDC/CTE-AST/098528/2008) and a Ciência 2007 fellowship. P.C. is grateful to F. Castelli, P. Bonifacio and L. Sbordone for their long term help with the SYNTHE and ATLAS12 codes. This publication has made use of the SIMBAD database, operated at CDS, Strasbourg, France.

References

Allende Prieto, C., Barklem, P. S., Lambert, D. L., & Cunha, K. 2004, A&A, 420, 183
Alonso, A., Arribas, S., & Martinez-Roger, C. 1996, A&A, 313, 873
Alonso, A., Arribas, S., & Martínez-Roger, C. 1999, A&AS, 140, 261
Arellano Ferro, A., & Mantegazza, L. 1996, A&A, 315, 542
Arellano Ferro, A., Parrao, L., Schuster, W., et al. 1990, A&AS, 83, 225
Árnadóttir, A. S., Feltzing, S., & Lundström, I. 2010, A&A, 521, A40
Barry, D. C., Cromwell, R. H., & Schoolman, S. A. 1978, ApJ, 222, 1032
Baumann, P., Ramírez, I., Meléndez, J., & Asplund, M. 2010, A&A, 519, A87
Bessell, M. S. 2005, ARA&A, 43, 293 (B2005)
Bessell, M. S., Castelli, F., & Plez, B. 1998, A&A, 333, 231
Blackwell, D. E., & Lynas-Gray, A. E. 1998, A&AS, 129, 505
Bohlin, R. C. 2007, in The Future of Photometric, Spectrophotometric and Polarimetric Standardization, ed. C. Sterken (San Francisco: ASP), ASP Conf. Ser., 364, 315
Bond, H. E. 1974, ApJ, 194, 95
Bond, H. E. 1980, ApJS, 44, 517
Bond, H. E., & Neff, J. S. 1969, ApJ, 158, 1235
Calamida, A., Bono, G., Stetson, P. B., et al. 2007, ApJ, 670, 400
Calamida, A., Bono, G., Stetson, P. B., et al. 2009, ApJ, 706, 1277
Casagrande, L., Portinari, L., & Flynn, C. 2006, MNRAS, 373, 13
Casagrande, L., Ramírez, I., Meléndez, J., Bessell, M., & Asplund, M. 2010, A&A, 512, A54
Castelli, F. 2005, Mem. Soc. Astron. Ital. Suppl., 8, 25
Castelli, F., & Kurucz, R. L. 2004 [arXiv:astro-ph/0405087]
Castelli, F., & Hubrig, S. 2004, A&A, 425, 263
Castelli, F., & Kurucz, R. L. 2006, A&A, 454, 333
Castelli, F., Gratton, R. G., & Kurucz, R. L. 1997, A&A, 318, 841
Cayrel de Strobel, G. 1996, A&A Rev., 7, 243
Cayrel de Strobel, G., Knowles, N., Hernandez, G., & Bentolila, C. 1981, A&A, 94, 1
Cayrel de Strobel, G., Soubiran, C., & Ralite, N. 2001, A&A, 373, 159
Chen, Y. Q., Nissen, P. E., Zhao, G., Zhang, H. W., & Benoni, T. 2000, A&AS, 141, 491
Chmielewski, Y. 1981, A&A, 93, 334
Clem, J. L., VandenBerg, D. A., Grundahl, F., & Bell, R. A. 2004, AJ, 127, 1227
Clements, G. L., & Neff, J. S. 1979, A&A, 75, 193
Coelho, P., Barbuy, B., Meléndez, J., Schiavon, R. P., & Castilho, B. V. 2005, A&A, 443, 735
Colina, L., Bohlin, R. C., & Castelli, F. 1996, AJ, 112, 307 (C96)
Conti, P. S., & Deutsch, A. J. 1966, ApJ, 145, 742
Cox, A. N. 2000, Allen's Astrophysical Quantities, 4th ed. (New York: AIP Press/Springer)
Crawford, D. L. 1966, Spectral Classification and Multicolour Photometry, 24, 170
Crawford, D. L. 1975, AJ, 80, 955
Crawford, D. L., & Mander, J. 1966, AJ, 71, 114
Crawford, D. L., & Barnes, J. V. 1970, AJ, 75, 978
Crawford, D. L., Barnes, J. V., Gibson, J., et al. 1972, A&AS, 5, 109
Croft, S. K., McNamara, D. H., & Feltz, K. A., Jr. 1972, PASP, 84, 515
Demarque, P., Woo, J.-H., Kim, Y.-C., & Yi, S. K. 2004, ApJS, 155, 667

Edvardsson, B. 2008, Phys. Scr., T133, 014011
Edvardsson, B., Andersen, J., Gustafsson, B., et al. 1993, A&A, 275, 101
Friel, E. D., & Boesgaard, A. M. 1992, ApJ, 387, 170
Gallouëtte, L. 1964, Ann. Astrophys., 27, 423
Gehren, T. 1981, A&A, 100, 97
Gratton, R. G., Carretta, E., & Castelli, F. 1996, A&A, 314, 191
Gray, D. F. 1992, PASP, 104, 1035
Gray, D. F. 1995, PASP, 107, 120
Gray, D. F. 2005, The Observation and Analysis of Stellar Photospheres, 3rd ed. (Cambridge, UK: Cambridge University Press)
Grønbech, B., Olsen, E. H., & Strömgren, B. 1976, A&AS, 26, 155
Grundahl, F., Vandenberg, D. A., Stetson, P. B., Andersen, M. I., & Briley, M. 2000, Liege Internat. Astrophys. Colloquia, 35, 503
Grundahl, F., Briley, M., Nissen, P. E., & Feltzing, S. 2002, A&A, 385, L14
Gustafsson, B. 2008, Phys. Scr., T130, 014036
Gustafsson, B., & Nissen, P. E. 1972, A&A, 19, 261
Gustafsson, B., Edvardsson, B., Eriksson, K., et al. 2008, A&A, 486, 951
Gustafsson, B., Meléndez, J., Asplund, M. & Yong, D. 2010, ApSS, 328, 185
Hauck, B., & Kunzli, M. 1996, Baltic Astron., 5, 303
Hauck, B., & Mermilliod, M. 1998, A&AS, 129, 431
Hardorp, J. 1978, A&A, 63, 383
Hardorp, J. 1980a, A&A, 88, 334
Hardorp, J. 1980b, A&A, 91, 221
Haywood, M. 2002, MNRAS, 337, 151
Haywood, M. 2008, MNRAS, 388, 1175
Hilker, M. 2000, A&A, 355, 994
Holmberg, J., Flynn, C., & Portinari, L. 2006, MNRAS, 367, 449
Holmberg, J., Nordström, B., & Andersen, J. 2007, A&A, 475, 519
Holmberg, J., Nordström, B., & Andersen, J. 2009, A&A, 501, 941
Israelian, G., García López, R. J., & Rebolo, R. 1998, ApJ, 507, 805
Johnson, H. L. 1962, ApJ, 135, 69
Johnson, H. L., Iriarte, B., Mitchell, R. I., & Wisniewski, W. Z. 1966, Comm. Lunar and Planetary Lab. (Tucson: Univ. of Arizona), 4, 99
Joner, M. D., & Taylor, B. J. 1995, PASP, 107, 124
Jonsell, K., Edvardsson, B., Gustafsson, B., et al. 2005, A&A, 440, 321
Karataş, Y., & Schuster, W. J. 2010, New Astron., 15, 444
Kron, G. E. 1963, PASP, 75, 288
Kuiper, G. P. 1938, ApJ, 88, 429
Kurucz, R. L. 1991, in Precision Photometry: Astrophysics of the Galaxy, ed. A. G. D. Philip, A. R. Upgren, & K. A. Janes (Schenectady, NY: Davis Press), 27
Kurucz, R. 1993, Diatomic Molecular Data for Opacity Calculations. Kurucz CD-ROM, Cambridge, Mass.: Smithsonian Astrophysical Observatory, 15
Kurucz, R. L. 1996, IAU Symp., 176, 523
Kurucz, R. L. 2005, Mem. Soc. Astron. Ital. Suppl., 8, 14
Kurucz, R. L., & Avrett, E. H. 1981, SAO Sp. Rep., 391
Lallement, R., Welsh, B. Y., Vergely, J. L., Crifo, F., & Sfeir, D. 2003, A&A, 411, 447
Lester, J. B., Gray, R. O., & Kurucz, R. L. 1986, ApJS, 61, 509
Lockwood, G. W., Tueg, H., & White, N. M. 1992, ApJ, 390, 668
Luck, R. E., & Heiter, U. 2006, AJ, 131, 3069 (LH06)
Magain, P. 1983, A&A, 122, 225
Malyuto, V. 1994, A&AS, 108, 441
Martell, S., & Laughlin, G. 2002, ApJ, 577, L45
Martell, S. L., & Smith, G. H. 2004, PASP, 116, 920
Meléndez, J., & Ramírez, I. 2003, A&A, 398, 705
Meléndez, J., & Ramírez, I. 2007, ApJ, 669, L89 (MR07)
Meléndez, J., Dodds-Eden, K., & Robles, J. A. 2006, ApJ, 641, L133 (M06)
Meléndez, J., Asplund, M., Gustafsson, B., & Yong, D. 2009, ApJ, 704, L66 (M09)
Meléndez, J., Casagrande, L., Ramírez, I., Asplund, M., & Schuster, W. J. 2010a, A&A, 515, L3
Meléndez, J., Ramírez, I., Casagrande, L., et al. 2010b, ApSS, 328, 193 (M10b)
Mermilliod, J.-C., Mermilliod, M., & Hauck, B. 1997, A&AS, 124, 349
Mironov, A. V., Moshkalev, V. G., & Kharitonov, A. V. 1998, Astron. Rep., 42, 799
Mitchell, R. I., & Schuster, W. J. 1985, AJ, 90, 2116
Neckel, H. 1986, A&A, 169, 194
Neckel, H. 1999, Sol. Phys., 184, 421 (N99)
Neckel, H. 2003, Sol. Phys., 212, 239 (N03)
Neckel, H., & Labs, D. 1981, Sol. Phys., 74, 231
Neckel, H., & Labs, D. 1984, Sol. Phys., 90, 205
Nissen, P. E. 1981, A&A, 97, 145
Nissen, P. E., & Schuster, W. J. 1991, A&A, 251, 457
Nordström, B., Mayor, M., Andersen, J., et al. 2004, A&A, 418, 989
Olsen, E. H. 1976, A&A, 50, 117
Olsen, E. H. 1983, A&AS, 54, 55
Olsen, E. H. 1984, A&AS, 57, 443
Önehag, A., Gustafsson, B., Eriksson, K., & Edvardsson, B. 2009, A&A, 498, 527 (O09)
Parrao, L., Schuster, W. J., & Arellano Ferro, A. 1988, Reporte Técnico, 52, Instituto de Astronomía, Universidad Nacional Autónoma de México
Pasquini, L., Biazzo, K., Bonifacio, P., Randich, S., & Bedin, L. R. 2008, A&A, 489, 677
Pettit, E., & Nicholson, S. B. 1928, ApJ, 68, 279
Porto de Mello, G. F., & da Silva, L. 1997, ApJ, 482, L89
Ramírez, I., & Meléndez, J. 2004, A&A, 417, 301
Ramírez, I., & Meléndez, J. 2005a, ApJ, 626, 446 (RM05a)
Ramírez, I., & Meléndez, J. 2005b, ApJ, 626, 465 (RM05b)
Ramírez, I., Meléndez, J., & Asplund, M. 2009, A&A, 508, L17 (R09)
Ramírez, I., Asplund, M., Baumann, P., Meléndez, J., & Bensby, T. 2010, A&A, 521, A33
Reddy, B. E., Tomkin, J., Lambert, D. L., & Allende Prieto, C. 2003, MNRAS, 340, 304
Relyea, L. J., & Kurucz, R. L. 1978, ApJS, 37, 45
Rieke, G. H., Blaylock, M., Decin, L., et al. 2008, AJ, 135, 2245
Saxner, M., & Hammarback, G. 1985, A&A, 151, 372
Sbordone, L., Bonifacio, P., Castelli, F., & Kurucz, R. L. 2004, Mem. Soc. Astron. Ital. Suppl., 5, 93
Sbordone, L., Bonifacio, P., Caffau, E., et al. 2010, A&A, 522, A26
Schuster, W. J. 1976, Rev. Mex. Astron. Astrofis., 1, 327
Schuster, W. J., & Nissen, P. E. 1988, A&AS, 73, 225 (SN)
Schuster, W. J., & Nissen, P. E. 1989, A&A, 221, 65
Schuster, W. J., & Parrao, L. 2001, Rev. Mex. Astron. Astrofis., 37, 187
Schuster, W. J., Parrao, L., & Contreras Martínez, M. E. 1993, A&AS, 97, 951 (SPC)
Schuster, W. J., Nissen, P. E., Parrao, L., Beers, T. C., & Overgaard, L. P. 1996, A&AS, 117, 317
Schuster, W. J., Parrao, L., & Guichard, J. 2002, J. Astron. Data, 8, 2
Schuster, W. J., Beers, T. C., Michel, R., Nissen, P. E., & García, G. 2004, A&A, 422, 527
Schuster, W. J., Moitinho, A., Márquez, A., Parrao, L., & Covarrubias, E. 2006, A&A, 445, 939
Secchi, A. 1868, Tip. Belle Arti, Roma, 68, tav. f. t.; OCCC 4 368 III
Sekiguchi, M., & Fukugita, M. 2000, AJ, 120, 1072
Smalley, B., & Dworetsky, M. M. 1995, A&A, 293, 446
Smalley, B., & Kupka, F. 1997, A&A, 328, 349
Soderblom, D. R., & King, J. R. 1998, in Solar Analogs: Characteristics and Optimum Candidates, ed. J. C. Hall (Flagstaff, Arizona: Lowell Observatory), 41
Soubiran, C., & Triaud, A. 2004, A&A, 418, 1089
Sousa, S. G., Santos, N. C., Mayor, M., et al. 2008, A&A, 487, 373 (S08)
Stebbins, J., & Kron, G. E. 1957, ApJ, 126, 266
Stebbins, J., & Whitford, A. E. 1945, ApJ, 102, 318
Straizys, V., & Valiauga, G. 1994, Baltic Astron., 3, 282
Strömgren, B. 1963, QJRAS, 4, 8
Strömgren, B. 1964, Astrophys. Norveg., 9, 333
Stromgren, B., Gustafsson, B., & Olsen, E. H. 1982, PASP, 94, 5
Takeda, Y., & Tajitsu, A. 2009, PASJ, 61, 471 (T09)
Takeda, Y., Kawanomoto, S., Honda, S., Ando, H., & Sakurai, T. 2007, A&A, 468, 663 (T07)
Taylor, B. J. 1984, ApJS, 54, 167
Taylor, B. J. 1994, PASP, 106, 444
Thuillier, G., Floyd, L., Woods, T. N., et al. 2004, Adv. Space Res., 34, 256
Tueg, H. 1982, A&A, 105, 395
Tueg, H., & Schmidt-Kaler, T. 1982, A&A, 105, 400
Twarog, B. A., Anthony-Twarog, B. J., & Tanner, D. 2002, AJ, 123, 2715
Twarog, B. A., Vargas, L. C., & Anthony-Twarog, B. J. 2007, AJ, 134, 1777
Valenti, J. A., & Fischer, D. A. 2005, ApJS, 159, 141 (VF05)
van den Bergh, S. 1965, JRASC, 59, 253
Vandenberg, D. A., & Bell, R. A. 1985, ApJS, 58, 561
Vandenberg, D. A., & Poll, H. E. 1989, AJ, 98, 1451
Welsh, B. Y., Lallement, R., Vergely, J.-L., & Raimond, S. 2010, A&A, 510, A54
Wielen, R., Fuchs, B., & Dettbarn, C. 1996, A&A, 314, 438
Woods, T. N., Prinz, D. K., Rottman, G. J., et al. 1996, J. Geophys. Res., 101, 9541
Yong, D., Grundahl, F., Johnson, J. A., & Asplund, M. 2008, ApJ, 684, 1159
Zacs, L., Nissen, P. E., & Schuster, W. J. 1998, A&A, 337, 216

Pages 12 to 15 are available in the electronic edition of the journal at http://www.aanda.org

Table 1. Photometry (*V* Johnson and *uvby*–β) of 73 solar-twin candidates from San Pedro Mártir Observatory.

HIP number	HD/BD number	V	$(b-y)$	m_1	c_1	N_V	N_{uvby}	β	N_β
348	225194	8.600	0.407	0.188	0.307	4	4	2.584	4
996	804	8.184	0.403	0.190	0.340	4	4	2.598	4
1411	1327	9.088	0.441	0.211	0.342	4	4	2.579	4
2894	+48 0182	8.653	0.415	0.208	0.291	4	4	2.587	4
4909	6204	8.508	0.403	0.206	0.319	4	4	2.597	4
5134	6470	8.965	0.402	0.187	0.281	4	4	2.581	4
6407	8291	8.612	0.411	0.205	0.296	4	4	2.584	4
7245	9446	8.377	0.423	0.218	0.328	4	4	2.596	4
8507	11195	8.890	0.413	0.207	0.317	4	4	2.595	4
8841	−13 0347	9.232	0.423	0.209	0.301	4	4	2.593	4
9349	12264	7.975	0.407	0.210	0.324	4	4	2.594	4
10710	+18 0289	8.924	0.400	0.191	0.302	5	5	2.594	5
11728	15632	8.041	0.414	0.219	0.333	5	5	2.590	5
11915	16008	8.608	0.406	0.211	0.314	4	4	2.594	4
14614	19518	7.858	0.400	0.198	0.303	5	5	2.591	5
18261	24552	7.976	0.390	0.195	0.325	5	5	2.604	5
25670	36152	8.285	0.413	0.219	0.380	6	6	2.599	6
28336	40620	8.982	0.411	0.209	0.294	6	6	2.578	6
35265	56124	6.936	0.395	0.207	0.349	7	7	2.594	7
36512	59711	7.732	0.403	0.210	0.316	5	5	2.588	5
38072	63487	9.206	0.406	0.215	0.351	6	6	2.601	6
41317	71334	7.808	0.409	0.218	0.341	5	5	2.588	5
41832	71779	8.125	0.399	0.199	0.322	7	7	2.580	7
42872	74645	9.276	0.402	0.198	0.363	4	4	2.594	4
44324	77006	7.942	0.390	0.190	0.322	6	6	2.587	6
44935	78534	8.722	0.413	0.212	0.344	5	5	2.590	5
44997	78660	8.346	0.412	0.221	0.322	5	5	2.588	5
47990	84705	8.704	0.406	0.218	0.327	5	5	2.591	5
49572	+30 1962	9.288	0.406	0.203	0.346	5	5	2.591	5
49756	88072	7.549	0.403	0.220	0.326	5	5	2.593	5
50826	+17 2213	9.129	0.403	0.189	0.283	5	5	2.581	5
51337	90733	8.905	0.399	0.203	0.354	5	5	2.595	5
52040	91909	9.194	0.406	0.207	0.288	5	5	2.573	5
52137	92074	8.638	0.415	0.218	0.317	5	5	2.584	5
55409	98649	8.010	0.407	0.217	0.356	5	5	2.585	5
55459	98618	7.658	0.406	0.206	0.341	5	5	2.607	5
58303	103828	8.443	0.411	0.210	0.314	5	5	2.642	5
59357	105779	8.665	0.389	0.189	0.318	5	5	2.581	5
60314	107633	8.783	0.409	0.213	0.362	4	5	2.592	5
60653	108204	8.737	0.401	0.181	0.352	5	5	2.579	5
63048	112257	7.808	0.423	0.220	0.351	5	5	2.582	5
64150	114174	6.795	0.412	0.234	0.335	5	5	2.584	5
64497	114826	8.943	0.411	0.215	0.351	5	5	2.598	5
64713	115169	9.268	0.398	0.211	0.355	5	5	2.579	5
64794	115382	8.433	0.408	0.201	0.321	3	3	2.584	3
64993	115739	8.899	0.405	0.213	0.341	3	3	2.588	3
65627	+47 2060	9.136	0.408	0.199	0.308	3	3	2.590	3
66885	119205	9.305	0.403	0.180	0.304	3	3	2.562	3
70394	+29 2529	9.568	0.431	0.226	0.305	4	4	2.580	4
73815	133600	8.198	0.409	0.212	0.328	4	5	2.600	5
74341	134902	8.861	0.416	0.214	0.335	3	3	2.588	3
74389	134664	7.781	0.395	0.214	0.392	3	4	2.590	4
75528	+47 2225	9.785	0.427	0.192	0.262	4	4	2.568	4
75923	138159	9.184	0.414	0.212	0.306	2	2	2.588	2
77883	142331	8.739	0.422	0.225	0.345	2	2	2.594	2
77936	234267	9.334	0.412	0.151	0.292	4	4	2.574	4
78028	+37 2687	8.640	0.410	0.185	0.307	4	4	2.590	4
78680	144270	8.198	0.404	0.182	0.299	4	4	2.594	4
79186	145514	8.316	0.427	0.185	0.322	4	4	2.583	4
79304	145478	8.684	0.412	0.192	0.359	4	4	2.594	4
79672	146233	5.494	0.400	0.219	0.356	4	4	2.603	4
81512	+45 2434	9.228	0.425	0.189	0.323	4	4	2.581	4
85285	157691	8.388	0.406	0.164	0.312	4	4	2.583	4

Table 1. continued.

HIP number	HD/BD number	V	$(b–y)$	m_1	c_1	N_V	N_{uvby}	β	N_β
88194	164595	7.070	0.415	0.195	0.336	4	4	2.591	4
88427	+35 3136	9.331	0.418	0.179	0.314	4	4	2.590	4
100963	195034	7.091	0.408	0.199	0.327	4	4	2.586	4
102152	197027	9.193	0.417	0.210	0.355	4	4	2.595	4
103025	+14 4456	8.719	0.414	0.190	0.353	4	4	2.587	5
104504	201422	8.550	0.396	0.191	0.305	4	4	2.589	5
108708	209096	8.943	0.415	0.217	0.353	4	4	2.595	4
108996	209562	8.894	0.406	0.209	0.345	4	4	2.598	4
109931	+24 4563	8.941	0.423	0.205	0.350	4	4	2.588	4
118159	224448	9.003	0.400	0.195	0.295	3	4	2.589	4

Table 2. Literature photometry (V Johnson and $uvby–\beta$) of solar-twin candidates and solar analogs (Mermilliod et al. 1997; Hauck & Mermilliod 1998).

HIP number	HD number	V	$(b–y)$	m_1	c_1	$N_{V,uvby}$	β	N_β
996	804	8.191	0.395	0.196	0.355	2		
11728	15632	8.035	0.414	0.221	0.335	3		
22263	30495	5.489	0.398	0.213	0.321	15	2.601	11
29525	42807	6.440	0.415	0.228	0.292	13	2.593	10
30502	45346	8.660	0.411	0.202	0.331	4		
36512	59711	7.742	0.406	0.204	0.308	2		
38228	63433	6.891	0.423	0.232	0.313	1		
41317	71334	7.812	0.412	0.210	0.327	4		
42438	72905	5.651	0.396	0.197	0.293	4	2.596	4
43190	75288	8.515	0.423	0.234	0.345	3		
44713	78429	7.303	0.414	0.227	0.348	3	2.600	19
44997	78660	8.345	0.410	0.216	0.321	2		
49756	88072	7.544	0.407	0.211	0.335	4		
55409	98649	8.004	0.405	0.227	0.323	1	2.588	1
55459	98618	7.658	0.411	0.198	0.347	2		
56948	101364	8.673	0.410	0.212	0.313	1		
64150	114174	6.791	0.419	0.231	0.334	15	2.592	9
77052	140538	5.869	0.424	0.231	0.334	5		
79672	146233	5.496	0.401	0.217	0.343	11	2.595	3
85042	157347	6.287	0.422	0.225	0.346	4		
100963	195034	7.090	0.408	0.204	0.319	1		
102152	197027	9.179	0.421	0.202	0.323	1		
109110	209779	7.581	0.415	0.216	0.318	2		
1499	1461	6.468	0.421	0.238	0.363	15	2.597	13
15457	20630	4.850	0.419	0.235	0.307	54	2.595	10
53721	95128	5.037	0.391	0.202	0.343	37	2.606	13
59610	106252	7.425	0.390	0.187	0.341	3		
60081	107148	8.021	0.424	0.244	0.394	2		
62175	110869	8.008	0.412	0.215	0.358	3		
79578	145825	6.563	0.395	0.228	0.328	1	2.597	1
80337	147513	5.373	0.399	0.199	0.323	5	2.609	1
96402	184768	7.556	0.426	0.214	0.343	6	2.590	6
96895	186408	5.979	0.410	0.212	0.370	64	2.606	39
96901	186427	6.234	0.416	0.223	0.352	63	2.597	39
113357	217014	5.456	0.416	0.232	0.371	143	2.603	13

Table 3. Stellar parameters.

HIP number	$T_{\rm eff}$	log g	[Fe/H]	Reference
348	5777	4.41	−0.13	R09
996	5860	4.38	0.00	R09
1499	5756	4.37	0.19	R09+VF05+LH06+T07+S08
2894	5820	4.54	−0.03	R09
4909	5836	4.44	0.02	R09
5134	5779	4.49	−0.19	R09
6407	5787	4.47	−0.09	R09
8507	5720	4.44	−0.08	R09
8841	5676	4.50	−0.12	R09
9349	5825	4.49	0.01	R09
10710	5817	4.39	−0.13	R09
11728	5738	4.37	0.05	R09+T07
11915	5793	4.45	−0.05	R09
14614	5803	4.47	−0.10	R09+T07+B10
15457	5771	4.56	0.08	B10+VF05
18261	5891	4.44	0.00	R09+T07
22263	5826	4.54	0.00	B10+VF05
25670	5755	4.38	0.07	R09+T07
28336	5713	4.53	−0.17	R09
29525	5715	4.41	0.00	B10
30502	5745	4.47	−0.01	M09
36512	5740	4.50	−0.09	M09+T07+S08
38072	5839	4.53	0.06	R09
38228	5693	4.52	0.01	R09+VF05
41317	5724	4.46	−0.04	M09+VF05+S08
42438	5864	4.46	−0.05	R09
43190	5775	4.37	0.12	M09
44324	5934	4.51	−0.02	R09+T07
44713	5784	4.36	0.10	B10+VF05+S08
44935	5800	4.41	0.07	M09
44997	5773	4.53	0.03	M09+T07
49572	5831	4.33	0.01	R09
49756	5804	4.45	0.04	R09+VF05+T07
50826	5725	4.47	−0.28	M09
52040	5785	4.51	−0.09	R09
52137	5842	4.56	0.07	R09
53721	5916	4.48	0.03	B10+VF05
55409	5760	4.52	−0.01	M09
55459	5838	4.42	0.04	R09+VF05+M06+MR07+T07
56948	5795	4.45	0.02	R09+MR07+T09+M10
59357	5810	4.45	−0.24	M09
59610	5899	4.34	−0.03	B10+VF05
60081	5811	4.38	0.32	M09+VF05+S08
60314	5874	4.52	0.11	R09
60653	5725	4.38	−0.29	M09
62175	5849	4.43	0.14	R09+T07
64150	5755	4.39	0.06	R09+VF05+T07
64713	5815	4.52	−0.01	M09
64794	5743	4.33	−0.10	R09
64993	5875	4.56	0.09	M09
66885	5685	4.48	−0.38	M09
73815	5803	4.34	0.02	MR07+R09
74341	5853	4.51	0.09	R09
74389	5859	4.48	0.11	M09+S08
75923	5775	4.56	−0.02	M09
77052	5697	4.54	0.04	B10+VF05
77883	5695	4.39	0.04	M09
79578	5860	4.53	0.07	M09+VF05
79672	5822	4.45	0.05	M09+VF05+M06+MR07+T07+T09+M09
80337	5881	4.53	0.03	B10+VF05+S08
85042	5692	4.39	0.04	B10+VF05+S08
85285	5730	4.43	−0.39	M09
88194	5735	4.40	−0.07	R09+VF05+T07
88427	5810	4.42	−0.16	R09
96402	5713	4.33	−0.03	B10+T07
96895	5808	4.33	0.10	R09+VF05+LH06
96901	5737	4.34	0.06	R09+VF05+LH06+T07
100963	5802	4.45	0.01	R09+T07+T09
102152	5737	4.35	−0.01	R09+M10b
104504	5836	4.50	−0.16	R09
108708	5875	4.51	0.15	R09
108996	5838	4.50	0.06	R09
109110	5817	4.46	0.06	B10+VF05+T07
109931	5739	4.29	0.04	R09
113357	5803	4.38	0.22	R09+VF05+LH06

Table 5. Solar colors and predictions from models atmospheres. Our synthetic colors (this work) were computed using the Bessell (2005) filters, with zero points based on both the STIS observed and ATLAS9 synthetic spectrum of Vega.

$(b–y)$	m_1	c_1	β	Reference
		Solar colors (this work)		
0.4105 (±0.0015)	0.2122 (±0.0018)	0.3319 (±0.0054)	2.5915 (±0.0024)	
		Solar spectra		
0.406,0.390(±0.004), $(b–y)$ from β			2.5955(±0.0024)	Olsen (1976), using asteroids
0.425	0.172	0.323	2.625	This work, C96 [STIS]
0.421	0.178	0.350	2.595	This work, C96 [ATLAS9]
0.424	0.188	0.306	2.632	This work, N99 [STIS]
0.420	0.194	0.333	2.602	This work, N99 [ATLAS9]
0.400	0.195	0.305	2.631	This work, N99+N03 [STIS]
0.396	0.201	0.332	2.601	This work, N99+N03 [ATLAS9]
0.402	0.225	0.287	2.625	This work, Thuillier (2004) [STIS]
0.398	0.231	0.314	2.595	This work, Thuillier (2004) [ATLAS9]
		Kurucz models		
0.371	0.214	0.243		Relyea & Kurucz (1978)
0.414				Kurucz (1991)
0.355, 0.388	0.235	0.359	2.618, 2.660	Lester et al. (1986)
			2.581	Smalley & Dworetsky (1995)
0.393(CM), 0.400(noOV), 0.414(OV)	0.278 (CM)	0.339 (CM)		Smalley & Kupka (1997)
0.397(noOVER), 0.410 (OVER)				Castelli et al. (1997)
			2.590	Castelli & Kurucz (2006)
0.410	0.208	0.276	2.617	This work, ATLAS9 [STIS]
0.406	0.214	0.303	2.587	This work, ATLAS9 [ATLAS9]
		MARCS models		
0.381	0.159	0.262		Vandenberg & Bell (1985)
0.383	0.258	0.325	2.589	O09
0.383	0.220	0.367	2.621	This work, MARCS 2008 [STIS]
0.379	0.226	0.394	2.591	This work, MARCS 2008 [ATLAS9]
		From empirical calibrations or average of solar analogs		
0.425(±0.015)				Gehren (1981)
0.407(±0.010)			2.591(±0.005)	Saxner & Hammarback (1985)
0.414(±0.003)				Gray (1992)
0.406(±0.004)				Edvardsson et al. (1993)
0.404(±0.005)				Cayrel de Strobel (1996)
0.3999	0.2090	0.323		Clem et al. (2004)
0.394				RM05b
0.403(±0.013)	0.200(±0.026)	0.370(±0.068)		Holmberg et al. (2006)
0.4089(±0.0100)				Casagrande et al. (2010)